

Chapter 2

Colloid Nanoparticles and Carbon Nanotubes. What Can We Learn About Their Biomedical Application From Molecular Dynamics Simulations?

Tomasz Panczyk, Lukasz Konczak and Pawel Wolski

Abstract The behavior of a multi-walled carbon nanotube functionalized by magnetic nanoparticles through triethylene glycol chains is studied using molecular dynamics simulations. Particular attention is paid to the effect of magnetic anisotropy of nanoparticles which significantly affects the behaviour of the system under external magnetic field. The magnetization reversal process is coupled with the standard atomistic molecular dynamics equations of motion by utilizing the Neel-Brown model. The overdamped Langevin dynamics is used for the description of the inertialess magnetization displacements. The key results obtained in this study concern: an energetic profile of the system accompanying transition of a magnetic nanoparticle from the vicinity of the nanotube tip to its sidewall, the range of the magnetic anisotropy constant in which the system performs structural rearrangements, and the release dynamics of cisplatin from the interior of the nanocontainer. Another analyzed architecture uses small gold nanoparticles linked with the nanotube by hydrazone bond containing fragments. Because hydrazone bonds hydrolyze at slightly acidic pH those gold nanoparticles become chemically disconnected from the CNT at such conditions. Thus, the previously encapsulated cisplatin molecules in the CNT inner cavity can be released only at acidic pH. Analysis of the above process at the molecular scale leads to the conclusion that the feasibility of such a mechanism can be canceled by strong dispersion forces existing between gold nanoparticles and CNT. However, the presence of cisplatin in the inner cavity of the carbon nanotube strongly reduces the range of dispersion interactions. The determined properties of the studied systems strongly suggest their application in the area of nanomedicine as drug targeting and delivery nanovehicles.

T. Panczyk (✉) · L. Konczak · P. Wolski

Jerzy Haber Institute of Catalysis and Surface Chemistry, Polish Academy of Sciences,
ul. Niezapominajek 8, 30-239 Krakow, Poland
e-mail: panczyk@vega.umcs.lublin.pl

© Springer International Publishing AG 2018

L. A. Bulavin and A. V. Chalyi (eds.), *Modern Problems of Molecular Physics*,
Springer Proceedings in Physics 197, https://doi.org/10.1007/978-3-319-61109-9_2

2.1 Introduction

Carbon nanotubes (CNT) and magnetic nanoparticles (MNP) are considered as materials of great importance in medical diagnosis or as drug carriers. Normally, the studies are focused on their individual applications rather than on their composites. But CNT-MNP composites reveal even more interesting properties though their fabrication might be a challenge in some cases. MNPs are widely applied as contrast agents in magnetic resonance imaging (MRI); however, there are many other medical applications of MNPs like *in vitro* bioseparation, drug delivery or hyperthermia [1–3]. Similarly, CNTs are currently recognized as very promising drug carriers acting either as molecular cargoes or as parts of drug-CNT composites enhancing pharmacological activity of the drugs [4–9].

CNTs possess many intriguing features that make them attractive drug delivery carriers. It is well-known that they experience the enhanced permeability and retention (EPR) effect [10]. The EPR effect enables CNTs to transport chemotherapeutic agents preferentially to tumor sites. However, this is not a specific property of CNTs as any nanoparticulate drug delivery system also experiences the EPR effect. A very specific property of CNTs is their needle-like shape which facilitates transmembrane penetration and intracellular accumulation of drugs via the “nano-needle” mechanism [11]. CNTs have also been shown to enter cells via energy-dependent endocytic pathways, [12] and display extraordinary ability for drug loading onto the surface or within the interior core of CNTs via both covalent and non-covalent interactions [13–16]. Finally, targeting molecules, such as folic acid, antibodies, and magnetic nanoparticles can be further incorporated onto the drug-loaded CNTs [17–20].

In our recent publications [21–23] many properties of carbon nanotubes functionalized by magnetic nanoparticles through triethylene glycol chains were carefully investigated. We discussed some key factors which provide the fundamental conditions for the creation of a functional nanocontainer (NC) being able to encapsulate drug molecules and perform drug release by applying an external magnetic field. However, successful fabrication of the magnetically triggered NC seems to be still a challenge because its proper function needs highly precise molecular structure.

Drug release from CNTs can be triggered in response to other chemical or physical factors. Particularly interesting seems to be the pH change from physiological 7.4 to an acidic one. It is well-known that tumor microenvironments reveal several specific properties which can be utilized for controlled drug release. The highly reducing environment of tumor cells, and pH reduction to ca. 5.5 due to lactic acid production caused by anaerobic glycolysis, were studied as triggering factors for the release of cisplatin from carbon nanotubes [24]. Irinotecan or doxorubicin were also studied as model drugs for acidic pH induced release of drugs from the inner cavities or surfaces of CNTs [5, 9, 25–27]. However, in the majority

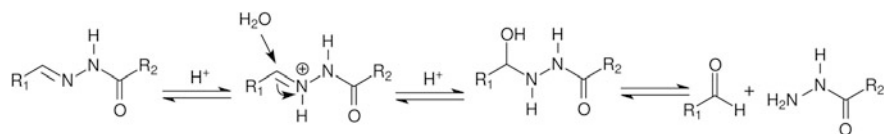


Fig. 2.1 Mechanism of hydrazone bond hydrolysis at acidic pH [28]

of cases the experimentally observed enhanced release of drugs at acidic pH is left without a deeper physical interpretation. For example, the pK_a of doxorubicin is ca. 8, so the observed enhanced release when the pH changes from 7.4 to 5.5 cannot be exclusively attributed to changes in the charge distribution or protonation of doxorubicin molecules.

In our theoretical studies of pH controlled drug delivery systems we applied a kind of reverse strategy. We constructed molecular architectures which have to be sensitive to pH in the discussed range. There are many chemical compounds which undergo structural transformations or even decomposition when pH drops from 7.4 to 5.5. One interesting example is hydrazone bond hydrolysis which occurs according to the scheme shown in Fig. 2.1 [28]. Thus, the application of hydrazone bonds fragments in the construction of pH sensitive drugs carriers is a very promising strategy since the hydrolysis phenomenon will occur precisely at tumor sites.

In this work we will discuss our observations concerning the system composed of a single-walled CNT and a gold nanoparticle functionalized by some chain molecules (linkers) containing hydrazone bond fragments [29]. To make a stable capped state of the CNT at neutral pH, the CNT tips were covalently linked with gold nanoparticles. However, the creation of the uncapped state upon hydrolysis of the hydrazone bonds turned out to be kinetically blocked. Therefore, theoretical analysis of such architecture on the molecular level helps to identify the most critical stages and point out which factors should be carefully optimized in order to make such a system fully functional.

2.2 Methods

The computational methodology utilized in this work is based on molecular dynamics simulations using the open source lammmps code [30]. The detailed description of the force field, including magnetic interactions, and computational approaches in the case of the magnetically triggered nanocontainer, can be found in our previous work [22, 23, 31]. The details of computational methodology and the force field applied to the model of pH triggered detachment of gold nanoparticles from the CNT tips is available in our recent work [29].

2.3 Results and Discussion

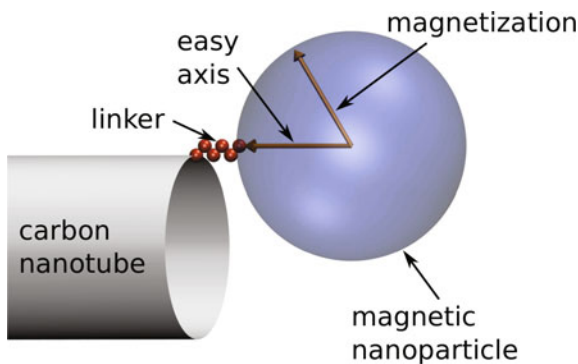
2.3.1 *Magnetically Triggered Nanocontainer*

2.3.1.1 Construction of a Functional Architecture

Our numerous theoretical studies of the magnetically triggered nanocontainer performed so far, led to several conclusions concerning the molecular structure of the functional system. The mechanism of its action is based on simple physical premises; however, a few conditions must be satisfied. Let us start from schematic representation of the system under investigation.

Figure 2.2 shows the key elements of the magnetically triggered nanocontainer. They consist of: (i) carbon nanotube; it may either be single-walled or multi-walled. In the case of a single-walled nanotube, the nanocontainer operates at milder conditions, however, in such a case the upper limit of the diameter of the SWCNT must be accounted for. Stable SWCNTs can reach diameters not larger than 2 nm which, in view of other conditions, is too little for construction of functional nanocontainers. Multi-walled nanotubes can have larger diameters but at the same time the dispersion interactions between the nanotube and magnetic nanoparticle become stronger and this implies application of a very hard magnetic material for the magnetic nanoparticles. (ii) linker; it may be any chain-like molecule but its chemistry must allow for covalent linking either with nanotube or with the magnetic nanoparticle. Its length is important—it cannot be too long. In our studies we used triethylene glycol chains. (iii) magnetic nanoparticle; such nanoparticles possess a magnetization vector and an easy axis of magnetization. Depending on the choice of magnetic material, the displacement of the magnetization vector from the easy axis direction needs various amounts of energy delivered by an external magnetic field. We found that the higher value of the magnetic anisotropy constant of the nanoparticle, the quicker the response of the nanocontainer to the magnetic field. Therefore, hard magnetic materials are preferred. In our studies we used material properties of metallic cobalt, and we found that a nanoparticle of 10 nm diameter is

Fig. 2.2 Scheme of the magnetically triggered nanocontainer



enough to obtain a sufficiently high magnetic anisotropy energy. Because fine metallic nanoparticles can undergo fast degradation in aqueous media, we considered the presence of a protective layer on the surfaces of the magnetic nanoparticles. That layer, made from e.g. alumina, reduces to some extent the range of dispersion interactions between the nanoparticle and the nanotube, and it also produces an electric charge on the nanoparticle due to electric double layer formation. That extra charge affects the total interaction energy with the nanotube because the carbon atoms on the nanotube tips can be saturated by other hydrophilic groups such as amines or carboxylates.

2.3.1.2 Basic Properties at Normal Conditions

Due to the significant range of the dispersion interactions acting between the CNT and the MNPs (both are extended bodies), and the presence of linker between them, the normal state of the nanocontainer is with the MNP adjacent to the CNT tips. We call this state the capped one. The stability of this state depends on factors such as the size of the system, the chemical nature of the MNP surface and its surface charge, the presence of functional groups on the CNT tips, and, to some extent, the length and chemical nature of the linker. In the capped state the total energy of the nanocontainer reaches a minimum, E_c , as shown in Fig. 2.3. The depth of this minimum can be controlled by adjustment of the parameters mentioned above.

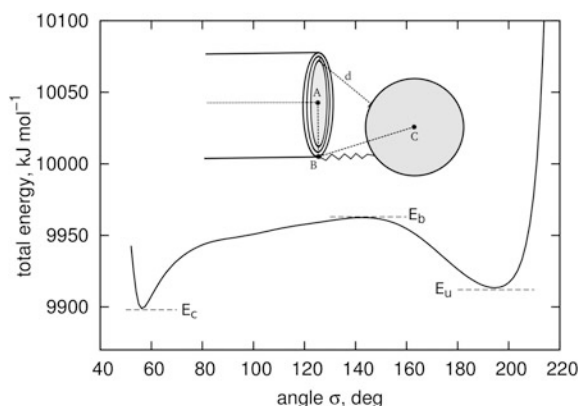


Fig. 2.3 Typical total energy profile of the nanocontainer associated with the transition of the magnetic nanoparticle from the nanotube tip to the sidewall (uncapping). E_c is the total energy minimum corresponding to the capped state, i.e. when the MNP adheres to the CNT tip, and E_u is the total energy minimum corresponding to the location of the MNP on the nanotube sidewall. E_b is the energy barrier separating these two minima. The total energy profile is plotted as a function of the angle σ which is defined by the coordinates of the points A, B and C shown in the inset. The section d is the distance between the surface of the MNP and carbon atoms located on the nanotube tip. It defines the degree of the uncapping

The preferred depth of the total energy minimum cannot be precisely determined but it should be “moderate”. This is because the capped state should be stable at normal conditions, and so $E_b - E_c$ should be greater than ca. $10 k_B T$. Very strong interactions in the capped state are, however, not preferred because that state cannot be thermodynamically locked and irreversible.

Looking at Fig. 2.3 we notice that the total energy of the system increases with the increasing value of the angle σ (which, in turn is correlated with the slit size d), passes the maximum E_b , and ends up in the second minimum E_u . This second minimum corresponds to localization of the MNP on the nanotube sidewall, i.e. we can call this state the uncapped one. The depth of the energy well in the uncapped state can be controlled by adjustment of exactly the same parameters as in the capped state. However, in this case the structure (state) of the CNT sidewall is very important. For example, the presence of some functional groups on the sidewalls can affect the interaction energy mainly in the uncapped state with only minor influence on the stability of the capped state.

These two energy minima are separated by the energy barrier E_b . This parameter is crucial for the proper function of the nanocontainer. As mentioned, E_b controls the kinetic stability of both the capped and uncapped states. Thus, the key factor in the design of the functional nanocontainer is a suitable adjustment of the energy barrier E_b .

2.3.1.3 Interaction with the External Magnetic Field

If the nanocontainer in the capped state is exposed to an external magnetic field then the magnetizations of the MNPs experience Néel rotation. Thus, they rotate in order to align with the direction of the field but at the same time they displace from the easy axes directions. This leads to appearance of magnetic anisotropy energy U_a according to the formula:

$$U_a = K_a V \sin^2 \theta \quad (2.1)$$

where K_a is the magnetic anisotropy constant of the material, V is volume of the magnetic core, and θ is the angle between magnetization vector and easy axis direction. The anisotropy energy creates a torque which drives the Brown rotation of the whole nanoparticle. However, at some point the linker between CNT and MNP hinders the Brown rotation. As a result, the MNP performs translation in order to minimize mismatch between the easy axis and magnetization directions. This translation leads finally to the uncapping of the nanotube.

Thus, the key factor responsible for the magnetically assisted uncapping of the nanocontainer is the magnetic anisotropy constant of the magnetic material. That parameter cannot be easily controlled as this is a material property. For example, the reported values of K_a for bulk metallic cobalt are $4.5 \times 10^5 \text{ J m}^{-3}$ and $2.5 \times 10^5 \text{ J m}^{-3}$ for hcp and fcc structures, respectively [32]. It is well known, however, that K_a is much larger for metal nanoparticles than for the bulk. For bulk samples, K_a is

primarily due to magnetocrystalline anisotropy whereas for nanoparticles the dominant contributions to the magnetic anisotropy arise from stresses, surface effects and the shape of the granules [33, 34]. Thus, for very small NPs consisting of about 30 Co atoms, the low-temperature value of K_a is $3 \times 10^7 \text{ J m}^{-3}$ i.e. two orders of magnitude larger than for bulk metal [34]. In other studies involving 40 Å cobalt NPs and temperatures about 600 K, it was found that $K_a = 6 \times 10^6 \text{ J m}^{-3}$ [35]. On the other hand, Respaud et. al. [32] found K_a in the range $0.83\text{--}1.0 \times 10^6 \text{ J m}^{-3}$ for ultrafine Co NPs (15 Å in diameter). As seen, the K_a value seems to be dependent on the NP sizes and probably also shape distribution and other factors that affect the values of K_a determined experimentally in different labs. Thus, it is difficult to predict a strict K_a value for a given case but knowing the above experimental values we can get a notion of the physically reasonable range of its values. The assumed diameter of magnetic cores in our model, 80 Å, is significantly larger than those mentioned above, thus we might expect that actual K_a values for our cobalt NPs should be rather closer to 10^6 J m^{-3} than to 10^7 J m^{-3} . Obviously cobalt is neither the only nor the best material for the magnetic caps of the NC. Materials based on rare earth elements often exhibit enormously high saturation magnetization and magnetic anisotropy. For example, SmCo_5 exhibits K_a value as high as $1.3 \times 10^7 \text{ J m}^{-3}$ for bulk material [36]. It is likely that SmCo_5 nanoparticles would possess a K_a value about one order of magnitude larger. Therefore, such materials represent reasonable alternatives if Co NPs revealed a magnetic anisotropy too low for proper function of the NC.

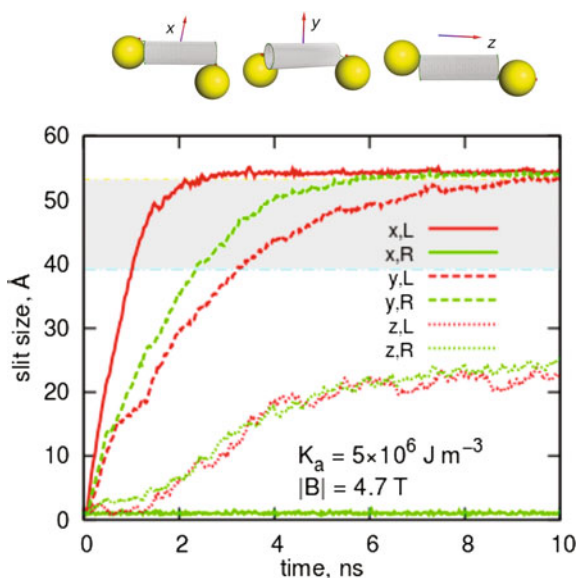
Figure 2.4 shows an example of the magnetically triggered uncapping of a nanocontainer which is composed of magnetic nanoparticles with a K_a value representative of cobalt, i.e. $5 \times 10^6 \text{ J m}^{-3}$. The strength of the external magnetic field was set to 4.7 T. This value produces the magnetic energy comparable to the anisotropy energy (2.1) and, as seen, it is enough to induce uncapping within times less than 10 ns. In Fig. 2.4 we also notice an important effect of the initial orientation of the nanocontainer with respect to the field direction. In some cases, when the orientation of the magnetization of a given nanoparticle is similar to the field direction, no uncapping occurs.

2.3.1.4 Spontaneous Recapping Without the External Magnetic Field

The uncapping transition involves overcoming an energy barrier, as mentioned in Sect. 2.3.1.2, and this can be done by exposing the system to an external magnetic field. The uncapped state is also separated by an energy barrier and that barrier can be significant. This means that the uncapping transition can be an irreversible process, however, this is not desirable. A functional nanocontainer should be able to spontaneously return to the capped state after some time. That property is necessary for drug loading prior to administration of the nanocontainer to the body.

As already mentioned, the energy barrier for the recapping transition can be controlled by modification of the nanotube sidewalls. We considered several methods, [23] however, the most promising seems to be covalent functionalization

Fig. 2.4 Magnetically triggered uncapping of the nanocontainer after exposure to a 4.7 T external magnetic field. The initial configuration was the fully capped structure brought to equilibrium without the external magnetic field applied. The magnetizations of the MNPs were aligned with the directions of the easy axes. The symbols x , y , and z mean the direction of the applied field. Codes L (left) and R (right) are used for formally distinguishing each end of the nanocontainer. The snapshots show the final configurations after 10 ns together with the indication of the magnetic field directions (arrows)



of the sidewall defect sites by other small functional groups. Table 2.1 shows selected results obtained by incorporation of amide groups on the sidewalls of triple-walled carbon nanotube.

As can be seen in Table 2.1, the energy barrier for the recapping of the bare triple-walled nanotube is about 72 kJ mol^{-1} . This is a relatively high (compared to $k_B T$) value and the recapping process will be very slow or it can even be kinetically blocked. It should be mentioned that MNPs are very heavy objects and their motion is orders of magnitude slower than atoms or molecules. Therefore, that value of the

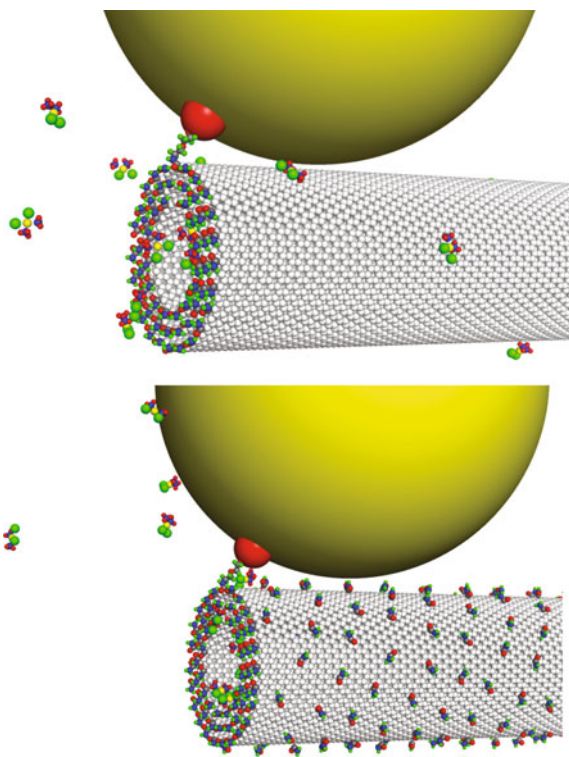
Table 2.1 Energy barriers found for the nanocontainer composed of triple-walled carbon nanotube, amide functionalized triple-walled carbon nanotube, and additionally filled with cisplatin molecules

Nanotube	Energy barrier for uncapping, kJ mol^{-1}	Energy barrier for recapping, kJ mol^{-1}
Bare triple-walled	107.8	72.4
Amide functionalized	116.8	52.1
Amide functionalized and filled in cisplatin	145.7	47.27

energy barrier means that the MNP is locked in the uncapped state of the nanocontainer. However, when the sidewall of the nanotube is functionalized by amide groups, the energy barrier drops by 20 kJ mol^{-1} . Our estimation of the likelihood of the recapping transition, based on the transition state theory, leads to the conclusion that barriers lower than ca. 60 kJ mol^{-1} can be overcome spontaneously within a reasonable timescale [23]. Thus, the covalent functionalization by amide groups seems to be a method of choice in the construction of a fully functional nanocontainer.

The presence of drug molecules in the inner cavity of the nanotube also affects the energetic picture of the nanocontainer. However, the encapsulated cisplatin molecules modify mainly the energy barrier for the uncapping transition. Also, the amide groups localized on the sidewalls enhance the energy barrier of the uncapping. This is due to an extra energy component coming from polar amide groups (bearing partial electric charges) distributed circularly around the MNP at the capped state. The cisplatin molecules also provide an extra energy component due to their interactions with the MNP in the capped state. The question is why those amide groups lower the energy barrier to the uncapped state. The answer comes

Fig. 2.5 Snapshots of the uncapped states of the nanocontainers composed of bare carbon nanotube (upper part) and amide functionalized nanotube (bottom part). In both cases, initially, the nanocontainers were filled in cisplatin molecules



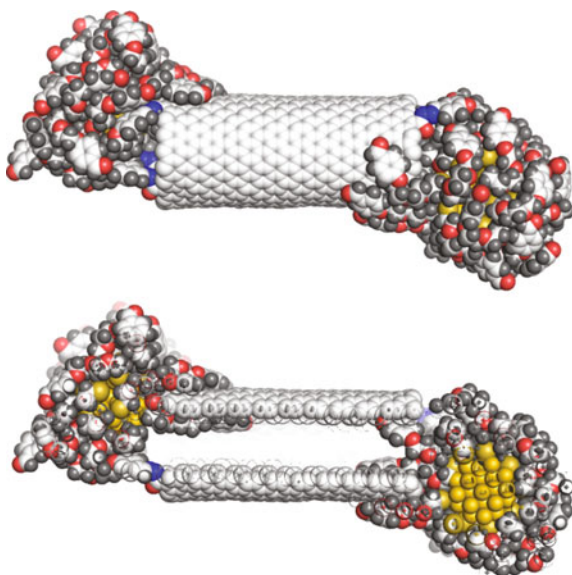
from analysis of the system snapshots with and without the presence of amide groups. As can be seen in Fig. 2.5, the attached amide groups prevent the MNP from a very close contact with the nanotube sidewall. This, in turn, reduces the range of the dispersion interactions between these two bodies. Therefore, the amide groups, or actually any other groups localized on the nanotube sidewall, act as steric obstacles. The snapshots in Fig. 2.5 also show that cisplatin quickly escapes from the CNT interior upon formation of the uncapped state.

2.3.2 *Uncapping of Carbon Nanotube by Detachment of Colloid Nanoparticles*

2.3.2.1 Bonded Form at Neutral PH

According to the scheme shown in Fig. 2.1, the hydrazone bonds are stable at neutral pH. Thus, we constructed a model system in which a single-walled carbon nanotube is linked with a gold nanoparticles by N'-[(E)-(4-{2-[2-(2-sulfanylethoxy) ethoxy] ethoxy} phenyl) methyldene] formic hydrazide linkers. The system is shown in Fig. 2.6 and it is stable at neutral pH by definition. Therefore, we focused mainly on the stability of the unbonded form at acidic pH.

Fig. 2.6 Simulation snapshot of a CNT functionalized by gold nanoparticles at neutral pH using the linkers N'-[(E)-(4-{2-[2-(2-sulfanylethoxy) ethoxy] ethoxy} phenyl) methyldene] formic hydrazide. The bottom part shows the cross-section of the system



2.3.2.2 Detachment of Gold Nanoparticles Upon Hydrolysis of Hydrazone Bonds

At acidic pH the hydrazone bonds are cleaved and gold nanoparticles are chemically disconnected from the CNT. Thus, we should observe detachment of gold nanoparticles from the CNT tips and release of previously encapsulated drug molecules from the CNT inner space. However, our calculation results concerning such systems led to the conclusion that gold nanoparticles do not detach from the CNT. A closer analysis of the system structure showed that some linkers, attached to gold nanoparticles, were incorporated in the internal space of the CNT, as shown in the inset of Fig. 2.7.

The presence of linkers in the CNT interior is the main factor responsible for the lack of detachment of gold nanoparticles from the CNT tips because the dispersion interactions between the hydrophilic nanoparticles and the hydrophobic CNT in such a small system should not be large. The potential of mean force (pmf), determined from biased simulations, reaches about 250 kJ mol^{-1} for the process of enforced separation of these two species (Fig. 2.7). Therefore, we can conclude that spontaneous detachment of gold nanoparticles from the CNT is thermodynamically impossible in the considered conditions.

However, an analysis of the system when the CNT interior is filled with cisplatin molecules gives the energy barrier against detachment not bigger than 15 kJ mol^{-1} (Fig. 2.8). This is not a big value and the spontaneous detachment and release of cisplatin should occur in normal conditions without any extra energy bias. Such a strong difference between the solvent filled CNT (Fig. 2.7) and cisplatin filled CNT

Fig. 2.7 Potential of mean force (pmf) determined while dragging the gold nanoparticle from the tip position to the bulk for the case when the interior of the nanotube is filled with solvent. The pmf was determined using the umbrella sampling method with weighted histogram analysis. The bottom snapshot shows a cross-section of the system in its initial position

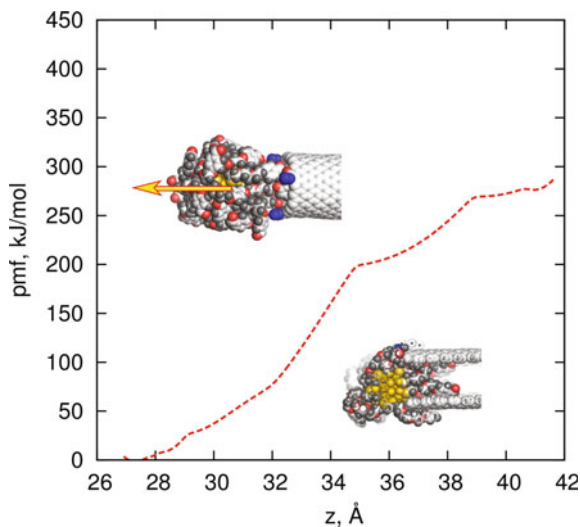
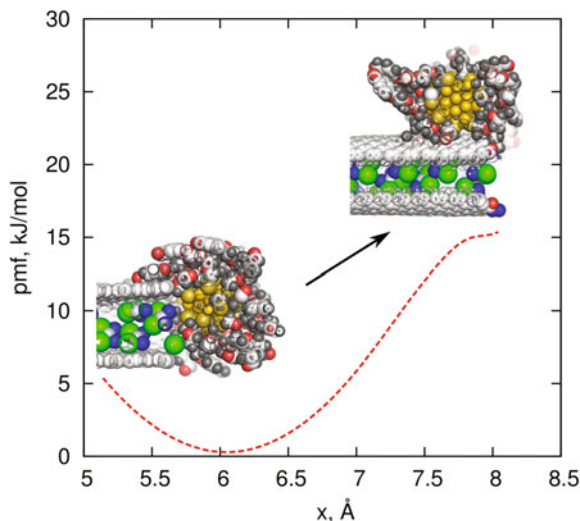


Fig. 2.8 Potential of mean force (pmf) determined while dragging the gold nanoparticle from the tip position to the sidewall for the case when the interior of the nanotube is filled with a mixture of cisplatin and solvent. The lefthand side snapshot shows the system structure in its initial position, while the righthand side shows the final position



(Fig. 2.8) is due to the lack of incorporation of linkers to the CNT interior in the latter case. Cisplatin forms a kind of condensed phase in the CNT internal space, and this prevents incorporation of linkers and reduces their anchoring effect.

2.4 Conclusions

Computer simulations are a valuable tool for predictions of how a particular molecular structure behaves under given conditions, and they can be used for the design of functional drug delivery systems. Magnetically controlled nanocontainers might be promising candidates as a drug targeting and delivery systems. They allow for high loadings of active component inside the nanotube and controllable release by means of an external magnetic field. However, they need a careful tuning of the molecular structure in order to obtain a proper energetic balance between the different states of the system. The presence of polar groups attached to the nanotube sidewalls makes the system fully functional, more hydrophilic, and reduces the risk of agglomeration of an ensemble of such systems into big clusters.

Hydrazone bond hydrolysis at slightly acidic pH is a promising factor for the construction of smart drug delivery systems. However, as shown in the analyzed system, there might appear some phenomena (difficult to predict in advance) which render the function impossible. In the particular case of capping the CNT by gold nanoparticles, we found that the incorporation of linkers in the CNT interior might lock the nanoparticles at the nanotube tips. Also, if bigger system sizes are considered, there might be a risk of locking the nanoparticles by dispersion interactions between the nanoparticles and the CNT.

Acknowledgements This work was supported by National Science Centre (NCN). Grant no. UMO-2012/07/E/ST4/00763.

References

1. S. Laurent, D. Forge, M. Port, A. Roch, C. Robic, L. Vander Elst, R.N. Muller, Magnetic iron oxide nanoparticles: synthesis, stabilization, vectorization, physicochemical characterizations, and biological applications. *Chem. Rev.* **108**, 2064–2110 (2008). <https://doi.org/10.1021/cr068445e>
2. M. Arruebo, R. Fernández-Pacheco, M.R. Ibarra, J. Santamaría, Magnetic nanoparticles for drug delivery. *Nano Today*. **2**, 22–32 (2007). [https://doi.org/10.1016/S1748-0132\(07\)70084-1](https://doi.org/10.1016/S1748-0132(07)70084-1)
3. K.A. Brown, C.C. Vassiliou, D. Issadore, J. Berezovsky, M.J. Cima, R.M. Westervelt, Scaling of transverse nuclear magnetic relaxation due to magnetic nanoparticle aggregation. *J. Magn. Magn. Mater.* **322**, 3122–3126 (2010). <https://doi.org/10.1016/j.jmmm.2010.05.044>
4. B.S. Wong, S.L. Yoong, A. Jagusiak, T. Panczyk, H.K. Ho, W.H. Ang, G. Pastorin, Carbon nanotubes for delivery of small molecule drugs. *Adv. Drug Deliv. Rev.* **65**, 1964–2015 (2013). <https://doi.org/10.1016/j.addr.2013.08.005>
5. H. Huang, Q. Yuan, J.S. Shah, R.D.K. Misra, A new family of folate-decorated and carbon nanotube-mediated drug delivery system: synthesis and drug delivery response. *Adv. Drug Deliv. Rev.* **63**, 1332–1339 (2011). <https://doi.org/10.1016/j.addr.2011.04.001>
6. D. Iannazzo, A. Piperno, A. Pistone, G. Grassi, S. Galvagno, Recent advances in carbon nanotubes as delivery systems for anticancer drugs. *Curr. Med. Chem.* **20**, 1333–1354 (2013). <https://doi.org/10.2174/0929867311320110001>
7. C.L. Lay, J. Liu, Y. Liu, Functionalized carbon nanotubes for anticancer drug delivery. *Expert Rev. Med. Devices* **8**, 561–566 (2011). <https://doi.org/10.1586/erd.11.34>
8. J. Li, S.Q. Yap, C.F. Chin, Q. Tian, S.L. Yoong, G. Pastorin, W.H. Ang, Platinum (iv) prodrugs entrapped within multiwalled carbon nanotubes: selective release by chemical reduction and hydrophobicity reversal. *Chem. Sci.* **3**, 2083 (2012). <https://doi.org/10.1039/c2sc01086k>
9. C. Tripisciano, M.H. Rummeli, X. Chen, E. Borowiak-Palen, Multi-wall carbon nanotubes—a vehicle for targeted Irinotecan drug delivery. *Phys. Status Solidi B* **247**, 2673–2677 (2010). <https://doi.org/10.1002/pssb.201000143>
10. H. Maeda, Macromolecular therapeutics in cancer treatment: the EPR effect and beyond. *J. Controlled Release* **164**, 138–144 (2012). <https://doi.org/10.1016/j.jconrel.2012.04.038>
11. A. Bianco, K. Kostarelos, C.D. Partidos, M. Prato, Biomedical applications of functionalised carbon nanotubes. *Chem. Commun. Camb. Engl.* 571–577 (2005). <https://doi.org/10.1039/b410943k>
12. N.W.S. Kam, Z. Liu, H. Dai, Carbon nanotubes as intracellular transporters for proteins and dna: an investigation of the uptake mechanism and pathway. *Angew. Chem.* **118**, 591–595 (2006). <https://doi.org/10.1002/ange.200503389>
13. Z. Ali Mohammadi, S.F. Aghamiri, A. Zarrabi, M.R. Talaie, A comparative study on non-covalent functionalization of carbon nanotubes by chitosan and its derivatives for delivery of doxorubicin. *Chem. Phys. Lett.* **642**, 22–28 (2015). <https://doi.org/10.1016/j.cplett.2015.10.075>
14. M. Bassioui, V.A. Basiuk, E.V. Basiuk, E. Álvarez-Zauco, M. Martínez-Herrera, A. Rojas-Aguilar, I. Puente-Lee, Noncovalent functionalization of single-walled carbon nanotubes with porphyrins. *Appl. Surf. Sci.* **275**, 168–177 (2013). <https://doi.org/10.1016/j.apsusc.2012.12.167>
15. H. Ismaili, F. Lagugné-Labarhet, M.S. Workentin, Covalently assembled gold nanoparticle-carbon nanotube hybrids via a photoinitiated carbene addition reaction. *Chem. Mater.* **23**, 1519–1525 (2011). <https://doi.org/10.1021/cm103284g>

16. Y.C. Jung, H. Muramatsu, T. Hayashi, J.H. Kim, Y.A. Kim, M. Endo, M.S. Dresselhaus, Covalent attachment of aromatic diisocyanate to the sidewalls of single- and double-walled carbon nanotubes. *Eur. J. Inorg. Chem.* **2010**, 4305–4308 (2010). <https://doi.org/10.1002/ejic.201000507>
17. A.R. Hilgenbrink, P.S. Low, Folate receptor-mediated drug targeting: from therapeutics to diagnostics. *J. Pharm. Sci.* **94**, 2135–2146 (2005). <https://doi.org/10.1002/jps.20457>
18. R. Li, R. Wu, L. Zhao, M. Wu, L. Yang, H. Zou, P-glycoprotein antibody functionalized carbon nanotube overcomes the multidrug resistance of human leukemia cells. *acs nano* **4**, 1399–1408 (2010). <https://doi.org/10.1021/nn9011225>
19. T. Panczyk, A. Jagusiak, G. Pastorin, W.H. Ang, J. Narkiewicz-Michalek, Molecular dynamics study of cisplatin release from carbon nanotubes capped by magnetic nanoparticles. *J. Phys. Chem. C* **117**, 17327–17336 (2013). <https://doi.org/10.1021/jp405593u>
20. F. Yang, C. Jin, D. Yang, Y. Jiang, J. Li, Y. Di, J. Hu, C. Wang, Q. Ni, D. Fu, Magnetic functionalised carbon nanotubes as drug vehicles for cancer lymph node metastasis treatment. *Eur. J. Cancer* **47**, 1873–1882 (2011). <https://doi.org/10.1016/j.ejca.2011.03.018>
21. T. Panczyk, T.P. Warzocha, Monte carlo study of the properties of a carbon nanotube functionalized by magnetic nanoparticles. *J. Phys. Chem. C* **113**, 19155–19160 (2009). <https://doi.org/10.1021/jp9062065>
22. T. Panczyk, M. Drach, P. Szabelski, A. Jagusiak, Magnetic anisotropy effects on the behavior of a carbon nanotube functionalized by magnetic nanoparticles under external magnetic fields. *J. Phys. Chem. C* **116**, 26091–26101 (2012). <https://doi.org/10.1021/jp3101442>
23. T. Panczyk, P. Wolski, L. Konczak, J. Narkiewicz-Michalek, Sidewall functionalization of carbon nanotubes as a method of controlling structural transformations of the magnetically triggered nanocontainer: a molecular dynamics study. *J. Phys. Chem. C* **119**, 8373–8381 (2015). <https://doi.org/10.1021/acs.jpcc.5b01155>
24. G. Pastorin, J. Li, S.L. Yoong, W.J. Goh, B.M.S. Czarny, Z. Yang, K. Poddar, M. Dykas, A. Patra, T. Thirumalai Venkatesan, C. Lee, T. Panczyk, In vitro controlled release of cisplatin from gold-carbon nanobottles via cleavable linkages. *Int. J. Nanomedicine*. 7425 (2015). <https://doi.org/10.2147/IJN.S93810>
25. Z. Ji, G. Lin, Q. Lu, L. Meng, X. Shen, L. Dong, C. Fu, X. Zhang, Targeted therapy of SMMC-7721 liver cancer in vitro and in vivo with carbon nanotubes based drug delivery system. *J. Colloid Interface Sci.* **365**, 143–149 (2012). <https://doi.org/10.1016/j.jcis.2011.09.013>
26. N.M. Dinan, F. Atyabi, M.-R. Rouini, M. Amini, A.-A. Golabchifar, R. Dinarvand, Doxorubicin loaded folate-targeted carbon nanotubes: Preparation, cellular internalization, in vitro cytotoxicity and disposition kinetic study in the isolated perfused rat liver. *Mater. Sci. Eng., C* **39**, 47–55 (2014). <https://doi.org/10.1016/j.msec.2014.01.055>
27. B. Anbarasan, S.V. Babu, K. Elango, B. Shriya, S. Ramaprabhu, pH responsive release of doxorubicin to the cancer cells by functionalized multi-walled carbon nanotubes. *J. Nanosci. Nanotechnol.* **15**, 4799–4805 (2015). <https://doi.org/10.1166/jnn.2015.9817>
28. J. Kalia, R.T. Raines, Hydrolytic stability of hydrazones and oximes. *Angew. Chem. Int. Ed.* **47**, 7523–7526 (2008). <https://doi.org/10.1002/anie.200802651>
29. T. Panczyk, L. Konczak, J. Narkiewicz-Michalek, G. Pastorin, Corking and uncorking carbon nanotubes by metal nanoparticles bearing ph-cleavable hydrazone linkers. theoretical analysis based on molecular dynamics simulations. *J. Phys. Chem. C* (2015). <https://doi.org/10.1021/acs.jpcc.5b08383>
30. S. Plimpton, Fast parallel algorithms for short-range molecular dynamics. *J. Comput. Phys.* **117**, 1–19 (1995). <https://doi.org/10.1006/jcph.1995.1039>
31. T. Panczyk, P. Szabelski, M. Drach, Implicit solvent model for effective molecular dynamics simulations of systems composed of colloid nanoparticles and carbon nanotubes. *J. Colloid Interface Sci.* **383**, 55–62 (2012). <https://doi.org/10.1016/j.jcis.2012.06.035>
32. M. Respaud, J.M. Broto, H. Rakoto, A.R. Fert, L. Thomas, B. Barbara, M. Verelst, E. Snoeck, P. Lecante, A. Mosset, J. Osuna, T.O. Ely, C. Amiens, B. Chaudret, Surface effects on the

- magnetic properties of ultrafine cobalt particles. *Phys. Rev. B.* **57**, 2925–2935 (1998). <https://doi.org/10.1103/PhysRevB.57.2925>
33. A. Gavrin, C.L. Chien, Fabrication and magnetic properties of granular alloys. *J. Appl. Phys.* **67**, 938 (1990). <https://doi.org/10.1063/1.346100>
 34. B.J. Hickey, M.A. Howson, D. Greig, N. Wiser, Enhanced magnetic anisotropy energy density for superparamagnetic particles of cobalt. *Phys. Rev. B.* **53**, 32–33 (1996). <https://doi.org/10.1103/PhysRevB.53.32>
 35. S. Gubin, Y. Spichkin, Y. Koksharov, G.Y. Yurkov, A. Kozinkin, T. Nedoseikina, M. Korobov, A. Tishin, Magnetic and structural properties of Co nanoparticles in a polymeric matrix. *J. Magn. Magn. Mater.* **265**, 234–242 (2003). [https://doi.org/10.1016/S0304-8853\(03\)00271-3](https://doi.org/10.1016/S0304-8853(03)00271-3)
 36. C.H. Chen, M.S. Walmer, M.H. Walmer, W. Gong, B.-M. Ma, The relationship of thermal expansion to magnetocrystalline anisotropy, spontaneous magnetization, and $T_{\text{sub c}}$ for permanent magnets. *J. Appl. Phys.* **85**, 5669 (1999). <https://doi.org/10.1063/1.369835>

<http://www.springer.com/978-3-319-61108-2>

Modern Problems of Molecular Physics

Selected Reviews from the 7th International Conference

"Physics of Liquid Matter: Modern Problems", Kyiv,

Ukraine, May 27–31, 2016

Bulavin, L.; Chalyi, A.V. (Eds.)

2018, XIV, 374 p. 156 illus., 100 illus. in color.,

Hardcover

ISBN: 978-3-319-61108-2